ELSEVIER

Chemical Engineering Journal 93 (2003) 11–22

Chemical Engineering Journal

www.elsevier.com/locate/cej

Preparation and characterization of Pd–Cu composite membranes for hydrogen separation

Fernando Roa [a], J. Douglas Way [a,*], Robert L. McCormick [a,1], Stephen N. Paglieri [b]

[a] *Department of Chemical Engineering, Colorado School of Mines, 1500 Illinois Street, Golden, CO 80401-1887, USA*
[b] *Los Alamos National Laboratory, P.O. Box 1663, MS-C348, Los Alamos, NM 87545, USA*

Abstract

Pd–Cu composite membranes were made by successive electroless deposition of Pd and then Cu onto various tubular porous ceramic supports. Ceramic filters used as supports included symmetric α-alumina (nominal 200 nm in pore size), asymmetric zirconia on α-alumina (nominal 50 nm pore size), and asymmetric γ-alumina on α-alumina (nominal 5 nm pore size). The resulting metal/ceramic composite membranes were heat-treated between 350 and 700 °C for times ranging from 6 to 25 days to induce intermetallic diffusion and obtain homogeneous metal films. Pure gas permeability tests were conducted using hydrogen and nitrogen. For an 11 μm thick, 10 wt.% Cu film on a nominal 50 nm pore size asymmetric ultrafilter with zirconia top layer, the flux at 450 °C and 345 kPa H_2 feed pressure was 0.8 mol/m^2 s. The ideal hydrogen/nitrogen separation factor was 1150 at the same conditions. The thickness of the metallic film was progressively decreased from 28 μm down to 1–2 μm and the alloy concentration was increased to 30 wt.% Cu.

Structural factors related to the ceramic support and the metallic film chemical composition are shown to be responsible for the differences in membrane performance. Among the former are the support pore size, which controls the required metal film thickness to insure a leak-free membrane and the internal structure of the support (symmetric or asymmetric) which changes the mass transfer resistance. The support with the 200 nm pores required more Pd to plug the pores than the asymmetric membranes with smaller pore sizes, as was expected. However, leak-free films could not be deposited on the support with the smallest pore size (5 nm γ-alumina), presumably due to surface defects and/or a lack of adhesion between the metal film and the membrane surface.

Keywords: Palladium; Copper; Palladium–copper alloy; Composite membrane; Electroless plating; Hydrogen separation; Gas separation; High temperature; Asymmetric ceramic supports

1. Introduction

The hydrogen separating capability of Pd alloy membranes is well known. Applications include hydrogenation and dehydrogenation reactions [1] and recovery of hydrogen from petrochemical plant streams [2]. Recently, there has been interest in utilization of Pd membranes to separate hydrogen produced in hydrocarbon reforming and coal gasification for power generation in fuel cells. Such applications have the potential to reduce energy consumption, capital costs or the number of unit operations compared to conventional systems. To consume less Pd, thin films or foils of Pd on the order of microns in thickness are applied to porous substrates for mechanical strength. Porous glass, ceramic, stainless steel, and polymers are common supports [3]. Hydrogen permeable metals such as tantalum (Ta) with a Pd coating also function as effective hydrogen separators [2,4].

Some very thin, permeable and permselective Pd composite membranes have been prepared by various research groups, although several hurdles inhibit commercial implementation of Pd membrane technology [5–7]. These problems include embrittlement and cracking due to the α → β Pd hydride phase transition, which occurs during temperature cycling [8] and poisoning or fouling due to the presence of sulfur or unsaturated carbon compounds in the operating stream [9–11]. Also, in order to be accepted by industry, membranes must have a lifecycle on the order of years under process conditions [12].

Alloys of Pd possess properties that may alleviate some of the shortcomings of pure Pd [13]. To begin with, the critical temperature for existence of the β phase hydride is lowered in alloys. This helps eliminate membrane rupture due to warping or cracking, a failure associated with temperature cycling. Many alloys are also more permeable to hydrogen

* Corresponding author. Tel.: +1-303-273-3519; fax: +1-303-273-3730.
E-mail addresses: dway@mines.edu (J.D. Way), robert_mccormick@nrel.gov (R.L. McCormick).
[1] Present address: NREL, 1617 Cole Blvd., Mail Stop 1633, Golden, CO 80401, USA.

1385-8947/02/$ – see front matter
PII: S1385-8947(02)00106-7

than pure Pd including $PdAg_{23}$ [14] (compositions in wt.%), $PdCu_{40}$ [15], PdY_7 [16,17] and $PdRu_7$ [18]. Alloys containing Au or Cu are more resistant to sulfur compounds [19,20]. Ternary and higher alloys of Pd have been developed to impart high temperature operating capability [21].

The hydrogen permeability of Pd–Cu passes through a maximum around 40 wt.% Cu significantly reducing membrane cost (relative to pure Pd), and this alloy exhibits increased resistance to H_2S [19,22–27]. Additionally, a b.c.c. alloy phase formed below 600 °C is credited with the increased permeability compared to pure Pd [26,28,29]. Like $PdAg_{23}$, $PdCu_{40}$ can withstand repeated temperature cycling with less distortion than pure Pd since at 40 wt.% Cu, the critical temperature for β-hydride phase formation is below room temperature [15,30–32].

Preparation of Pd alloys has been accomplished in the past by casting and rolling or induction melting followed by cold working into a foil or tube [33–35]. Composite Pd alloy membranes have been fabricated by sputtering, CVD, electroplating, and electroless plating. Much recent work has involved the use of electroless plating to make Pd–Ag [36–39], Pd–Ni [40] and Pd–Au alloy membranes [41].

Pd–Ag alloy films have been fabricated by several research groups using sequential metal deposition followed by annealing [39,42,43]. To obtain a homogeneous alloy film from two distinct metal layers in a reasonable amount of time, a high enough temperature must be utilized to promote complete intermetallic diffusion [38]. Shu et al. [37] annealed a *codeposited* Pd–Ag film for 150 min at 400 °C and a *sequentially* deposited Pd–Ag film for 5 h at 700 °C, while Kikuchi [39] annealed a sequentially deposited Pd–Cu film between 300 and 540 °C. Kikuchi and Uemiya [44] deposited Pd–Ag alloy films by sequential electroless plating, followed by heat treatment at temperatures of 800–1300 °C. Uemiya et al. [38] found that Pd–Ag films deposited by sequential electroless deposition require high temperatures (>800 °C) to produce a homogeneous film. Sakai et al. [43] and Kawae et al. [45] annealed Pd–Ag at 900 °C for 2 and 12 h, respectively.

Lin and coworkers [46–48] have deposited Pd–Ag films onto asymmetric γ-alumina supports (3 nm pores) using magnetron sputtering. A membrane with a 177 nm $PdAg_{18}$ film exhibited hydrogen/helium permselectivity of 3845 at 300 °C [48]. An observation they made was that the beginning surface roughness of the support was a critical parameter in obtaining a defect-free and adherent membrane [46].

Deposition under an osmotic pressure gradient by conducting electroless plating with a more concentrated solution on the opposite side of the porous support has been found to produce thinner Pd films that are more impenetrable to permeation of gases other than hydrogen [49,50]. Several desirable features of applying this technique to the manufacture of the Pd–Cu membranes include smaller grain-size, reduction in porosity, surface homogeneity and densification of the plated film.

Most Pd–Cu alloy membrane work has been carried out using foils [15,17,26,51]. Apparently, the only group to previously fabricate Pd–Cu alloy films on porous supports by electroless deposition of Pd and then Cu with subsequent annealing (500 °C for 12 h) was Kikuchi and coworkers [38,39]. The objective of the present work was to fabricate a thin and hydrogen selective Pd–Cu composite membrane in a similar fashion while reducing the thickness of the metal film. Three different types of tubular, porous ceramic membranes with progressively smaller pore sizes were used as supports for the thin Pd–Cu films. The effect of film thickness and composition on annealing conditions and hydrogen permeability was also investigated.

2. Experimental section

2.1. Support specifications

Tubular, porous alumina microfilters with nominal 0.2 μm pore size, were procured from Golden Technologies Company (now Coors Tech Oak Ridge, Oak Ridge, Tennessee). Designated GTC998, these tubes have an OD of 9 mm, an ID of 6.1 mm, and are fabricated from 99.8% pure α-alumina. Fig. 1 is a scanning electron microscope (SEM) image of the GTC998 cross-section. Asymmetric ceramic membranes consisting of a sol–gel zirconia selective layer on top of several porous support layers composed of α-alumina particles were also used. The other asymmetric membranes used in this work had nominal 5 nm pore size with a γ-alumina selective layer coated on top of the two layers with pore sizes of 0.4 and 0.2 μm (α-alumina) on the same type of macroporous support. Asymmetric supports were purchased from the U.S. Filter Corporation (Palm Desert, CA). A scanning

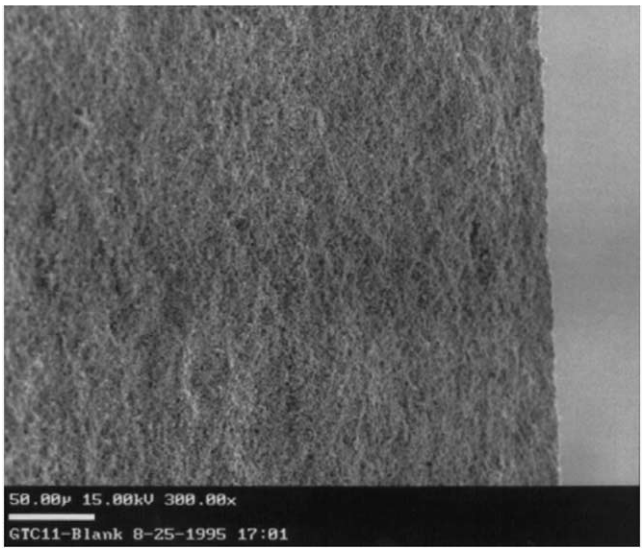

Fig. 1. Cross-section of symmetric, α-alumina GTC998 support with a nominal 0.2 μm pore size. Scalebar is 50 μm.

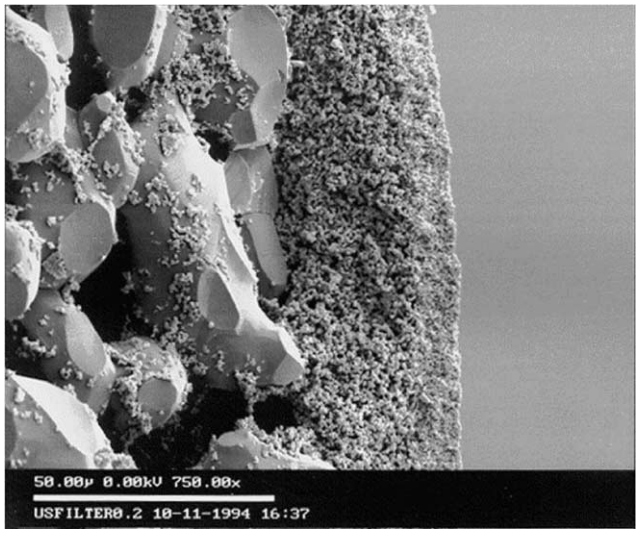

Fig. 2. Cross-section of an asymmetric, alumina ultrafilter. Scalebar is 50 μm.

electron micrograph of the cross-section of a typical asymmetric alumina membrane is shown in Fig. 2.

2.2. Substrate preparation

The detailed procedure for substrate preparation has been given elsewhere [52,53]. Selected support tubes were cut to length with a diamond saw, sequentially cleaned and rinsed ultrasonically in solutions of Alconox detergent, acetic acid, hot water, and 2-propanol [52]. After cleaning, the ends of the ceramic tubes were sealed with a high temperature glaze.

2.3. Surface activation

The surface activation step has been described in detail by Paglieri et al. [53]. Briefly, the support tube was dip-coated for 3 min in a 0.05–0.2 M solution of Pd acetate in chloroform, dried, calcined at 400 °C and hydrotreated at 450 °C for 2 h, followed by cooling under hydrogen.

2.4. Metal film deposition

The plating methodology to produce a Pd–Cu alloy film has been described in detail by Paglieri [54]. In summary, the preparation of a Pd–Cu alloy membrane film can be divided into two distinct steps, electroless plating of Pd and Cu followed by high temperature annealing in flowing H_2. First, layers of Pd and Cu were sequentially deposited by electroless plating on activated porous substrates. The plating time and gravimetric analysis were used to approximately determine the final alloy composition. The electroless palladium and copper plating bath recipes are reported in Table 1. It was found that electroless plating of Cu onto a Pd/alumina composite membrane was necessary because otherwise the electroless Pd solution replaced Cu by displacement plating. The plating bath temperature was controlled to 65±5 °C in a water bath. Plating cycle time was adjusted to achieve the desired Pd-layer thickness. After plating, the membranes were rinsed, soaked for several hours to overnight in 70 °C water (to remove plating solution and other impurities), rinsed, dried in air at 80 °C, and weighed. The Pd film thickness was estimated by dividing the weight difference between the plated and unplated membrane by the plated surface area and density of Pd (11.96 g/cm^3). Scanning electron microscopy was also used to determine film thickness following permeation measurements. Finally, the composite membrane was annealed above 350 °C in hydrogen to form a homogeneous alloy.

Table 1
Electroless Pd and Cu plating baths

Solution	Constituent	Quantity
Pd plating bath	$PdCl_2$, 99.9% pure	5.45 g/l
	NH_4OH	389.6 ml/l
	Na_2EDTA	70 g/l
	N_2H_4 (1.0 M)	10 ml/l
	HCl	10.9 ml/l
Cu plating bath	$CuSO_4$	6.225 g/l $CuSO_4{\cdot}5H_2O$
	Na_2EDTA	20.0988 g/l
	Formaldehyde (37%)	14.039 ml/l
	NaOH	20 g/l
	Triton X-100	25 mg/l
	2,2-bipyridyl	5 mg/l

2.5. High temperature testing procedures

Gas permeation experiments began with a room temperature leak test conducted with nitrogen, followed by high temperature gas permeation experiments conducted with hydrogen and nitrogen. The room temperature leak test was conducted in the following manner: the membranes were sealed into stainless steel compression fittings with graphite ferrules, the lumen was pressurized with nitrogen at 896 kPa and submerged in an alcohol/water mixture. The time for the pressure to drop to 827 kPa was measured and an unsteady state mass balance was solved to yield the room temperature nitrogen flux through the membrane:

$$J_{N_2} = \frac{D_m}{4RTt} \ln\left[\frac{P_1 - P_0}{P_2 - P_0}\right](P_2 - P_0) \quad (1)$$

where J_{N_2} is the nitrogen leak flux, D_m the internal tube diameter, R the universal gas constant, T the temperature, P_1 the initial pressure, P_2 the final pressure, P_0 the atmospheric pressure and t the time for the pressure to drop from P_1 to P_2. Calculated N_2 fluxes are reported in Table 2.

Following the leak test, permeation tests were performed at high temperature. The membrane was loaded into a stainless steel shell and centered in a tube furnace. The permeation module design is described in detail in a prior

Table 2
Room temperature leak testing of Pd–Cu membranes

Membrane no.	Type of support material	Support pore size (nm)	Estimated thickness of Pd film	N_2 flux[a] (mol/m^2 s) $\times 10^4$	Estimated thickness of Cu film	N_2 flux[b] (mol/m^2 s) $\times 10^4$
1	Symmetric α-alumina	200	47	–	10	–
2	Symmetric α-alumina	200	10	3.15	4	0.94
3	Symmetric α-alumina	200	6.5	1.45	4	0.47
4	Symmetric α-alumina	200	8	1.16	8	0.29
5	Asymmetric zirconia	50	8	0.30	6	0.25
6	Asymmetric zirconia	50	1.5	0.44	1	0.32
7	Asymmetric γ-alumina	5	10	very high	–	–

[a] The membrane, coated with Pd, is pressurized with N_2 at 896.3 kPa. The time for the pressure to drop at 827.4 kPa is measured and the flux calculated.
[b] As above but now the membrane is coated with both Pd and Cu.

publication [52]. Single-gas permeability tests were conducted at transmembrane pressure differentials of either 345 or 690 kPa using either hydrogen or nitrogen up to 700 °C. Brooks mass flow controllers metered gas flow or it was controlled manually with a needle valve. All gases were nominally 99.999% pure (UHP grade) and were used without further purification. The permeate pressure (shell side) was local atmospheric pressure (∼83 kPa). No sweep gas was used on the permeate side during the single-gas permeation experiments. Gas flow rates were measured using bubble flowmeters. These values were converted to STP and pure gas fluxes were calculated. The sweep side was purged with helium after testing with hydrogen, otherwise back-permeation of hydrogen to the tube side through the membrane resulted in a negative flux for a period of time.

The membrane was heated (and cooled) at 1 °C/min under helium purge. To avoid embrittlement of the pure Pd films, hydrogen was not introduced until 350 °C, well above the critical temperature for the α → β phase transition [13] for pure Pd. In some instances, while conducting the permeability tests, the membranes were exposed to flowing air at 275 kPa for 30 min. This procedure seems to enhance the hydrogen permeation through rearrangement of the metal surface [55].

Upon completion of high temperature permeability tests, the membrane was cooled at 1 °C/min under inert gas. Final measurements of inert gas flux through the membrane were then made at room temperature. After removal of the membrane from the permeation apparatus, it was visually inspected to determine if leaks originated from the membrane or the fittings by performing another ambient temperature leak test under isopropanol/water.

2.6. Membrane characterization

The tested membranes were frozen in liquid nitrogen and then fractured into small pieces, acceptable for instrumental analysis. Scanning electron microscopy (SEM-JEOL 840) was used to study film morphology and estimate Pd film thickness. Specimens were prepared by attaching pieces of broken membrane to metal buttons with carbon paint or tape. The samples were coated with gold (thickness of gold coating ∼5 pm) to make them more conductive. Then the film morphology was observed by scanning over large portions of the film surface and cross-section at both low and high magnifications. Metal film thicknesses were obtained by averaging measurements made from several micrographs taken at different locations perpendicular to the cross-section.

Pd–Cu alloy structure and domain orientation were examined by X-ray diffraction (XRD-Rigaku RU-200). Metal films were first peeled off from the ceramic substrate and then mounted on glass slides using double-sided tape. Scanning was typically conducted over the angular range from 20° to 90° 2θ. Energy-dispersive X-ray analysis (EDAX-Noran 5500) was used for elemental analysis. Samples were prepared the same as those for SEM but coated with carbon instead of gold for elemental analysis.

3. Results and discussion

3.1. Annealing

The objective of this part of the work was to prove that alloys of Pd and Cu could be prepared in situ by heating successively electrolessly deposited layers of each metal. The literature provides wide support to this hypothesis [27,38,39]. From the Pd–Cu phase diagram, Pd and Cu are miscible over the entire range of compositions, so their intermixing should take place with relative ease [56].

Small pieces of GTC Pd–Cu Membrane were heated to 600 °C for 12 h under helium and analyzed afterwards with XRD to determine if a homogeneous film was created. The XRD analysis of the metal films (Fig. 3) demonstrated that an alloy membrane was formed upon heat treatment at 600 °C in comparison to the unheated sample. Small amounts of non-annealed copper are still observed; however, additional annealing is accomplished during H_2 permeation testing. EDAX analysis of membranes after testing has always shown uniform Cu and Pd concentration profiles as shown in Figs. 6b and 8b. Those results demonstrated the potential for Pd–Cu membranes to be prepared by sequential electroless deposition followed by in situ annealing at high

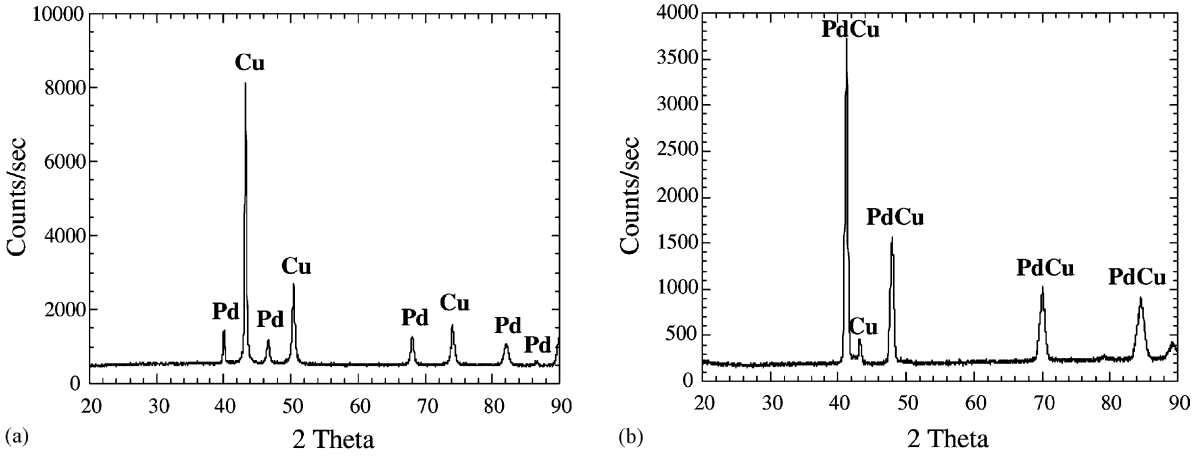

Fig. 3. XRD results for the annealing of GTC Pd–Cu membrane. Film thickness ≅ 22 μm. (a) As electrolessly deposited; (b) annealed at 600 °C for 12 h under helium.

temperature. Subsequent membranes were all heat-treated while carrying out the hydrogen transport measurements at the same time.

3.2. Influence of supports

Two important structural factors were considered in selecting the supports: pore size and symmetry. Their influence on the membrane performance is fundamental in establishing an understanding of how the support affects membrane fabrication and performance. These include the minimum thickness of a leak-free metal film and the overall mass transfer resistance. Regarding the former, our conjecture was that a support having a smoother surface (small pore size) would require a thinner film of metal to be leak-free. For the second, our proposition was that asymmetric supports when combined with the metal film should present less resistance to the hydrogen flux than symmetric tubes.

In order to address these hypotheses, different types of supports with varied structural features were used to make the Pd–Cu composite membranes, which were later annealed and tested according to the procedure described before. Table 3 presents the high temperature gas permeation results for all the membranes tested.

3.3. Symmetric supports

Initial experiments were performed using symmetric α-Al_2O_3 tubes, 200 nm in pore size. Early trials using these supports suggested that palladium deposition alone was sufficient to plug the pores. For instance, when a leaking Pd-coated tube was plated with copper, it routinely continued leaking. In general, palladium plating times of several hours were required for these symmetric tubes before leak-free membranes were obtained. Consequently, thicker layers of metal were deposited in comparison with the asymmetric tubes as shown in Table 2. This behavior indicates that the pore size basically controls how thick the metal film has to be to guarantee a low leakage rate.

Fig. 4 presents the high temperature permeation test results for membrane 1. With a thickness close to 30 μm, this membrane produced a maximum ideal separation factor H_2/N_2 of 14 and a hydrogen flux of roughly 0.05 mol/m^{2}s. An XRD analysis on that membrane revealed the formation of a Pd–Cu alloy containing 24 wt.% copper [54].

Using the same kind of support, three more membranes were fabricated reducing the palladium plating time to determine the minimum metal film thickness required. In Table 3, details for membranes 2–4 are presented. Membrane 3 was

Table 3
Summary of Pd–Cu membrane performance and characterization

Membrane no.	ΔP (kPa)	Heated to (K)	H_2 flux at 500 °C (mol/m^2 s)	Highest selectivity[a]	Thickness from SEM (μm)	Pd–Cu from EDAX (wt.%)
1	689.5	723	0.048	14	27.6 ± 8.5	72–28
2	344.7	973	0.35	70	11.0 ± 1.0	80–20
3	344.7	773	0.52	170	11.6 ± 1.0	81–19
4	344.7	723	0.18[b]	270	12.5 ± 1.5	78–22
5	344.7	723	0.80	1400	12 ± 1.0	91–9
6	344.7	723	0.66[c]	47	1.5 ± 0.2	70–30

[a] Selectivity = hydrogen flux/nitrogen flux.
[b] Measurement made at 450 °C.
[c] Measurement made at 350 °C.

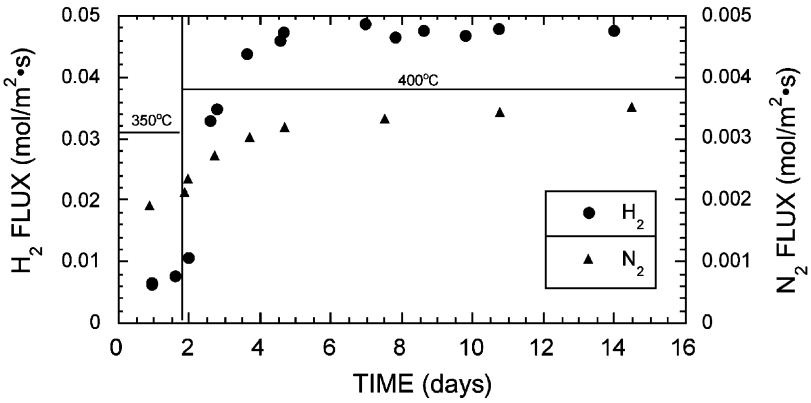

Fig. 4. Flux data for membrane 1. Film thickness ≅ 30 μm. The pressure differential for permeation tests was 690 kPa.

chosen as most representative for those three. Fig. 5 represents the high temperature permeation test for this membrane; Fig. 6 shows a detailed SEM section of the metal layer upon which EDAX elemental analysis was carried out.

Clearly, improvements in the separation factor and the hydrogen flux through the membrane were achieved. As seen in Table 3, an average separation factor of 170 and a H_2 flux of over eight-and-a-half times that for membrane 1 were obtained using just one-third of the thickness in the latter. The EDAX concentration plot indicates the presence of copper throughout the palladium film but at slightly higher concentration close to the gas–metal interface. Similar EDAX patterns were obtained for membranes 2 and 4, proving that alloying in situ had worked as proposed and the Cu composition profile was essentially uniform.

The increase in the separation factor can be attributed to the fine tuning of plating parameters including bath temperature, flow rates and overall hydrodynamics of the plating setup. These allowed more stable and homogeneous plating, which in turn created a more impervious film. On the other hand, smaller metal film thicknesses, a result of less plating time, were the cause of higher hydrogen fluxes since the metal layer provides the major mass transfer resistance; [7,57]. However, an acceptably low nitrogen leakage rate could not be obtained for any of these membranes if the thickness was less than about 11 μm. As pointed out before, to further decrease the thickness of the metal film, a support having smaller pore size in the top layer (less surface roughness) had to be used.

3.4. Asymmetric supports

Membranes 5 and 6 were made using an asymmetric support, whose selective porous top layer was 50 nm in pore size. We hypothesized that the thickness of metal layer needed to make a leak-free membrane on these supports should be greatly diminished. In general, this strategy was confirmed and successful in achieving better membrane performance as seen in Table 3.

Membrane 5, in particular, exhibited very high separation factor and hydrogen flux in spite of having about the same thickness as membranes 3 and 4. Fig. 7 shows the high temperature permeation experiments and Fig. 8 the membrane's EDAX quantitative elemental analysis with respective SEM detail. A very homogeneous Pd–Cu film can be observed, containing about 10% Cu.

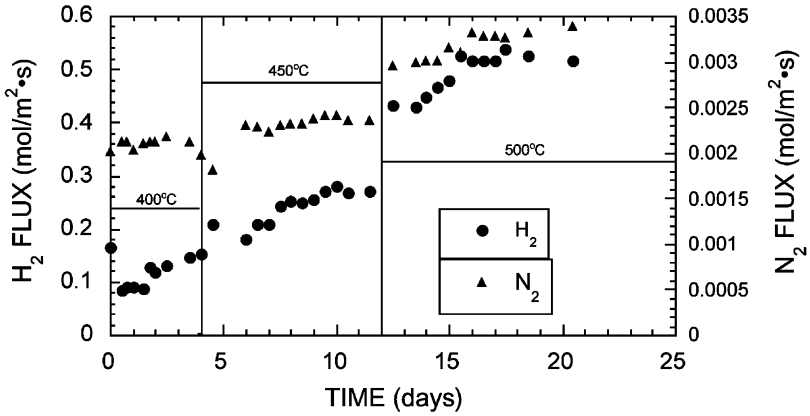

Fig. 5. Flux data for membrane 3. Film thickness ≅ 11 μm. The pressure differential for permeation tests was 345 kPa.

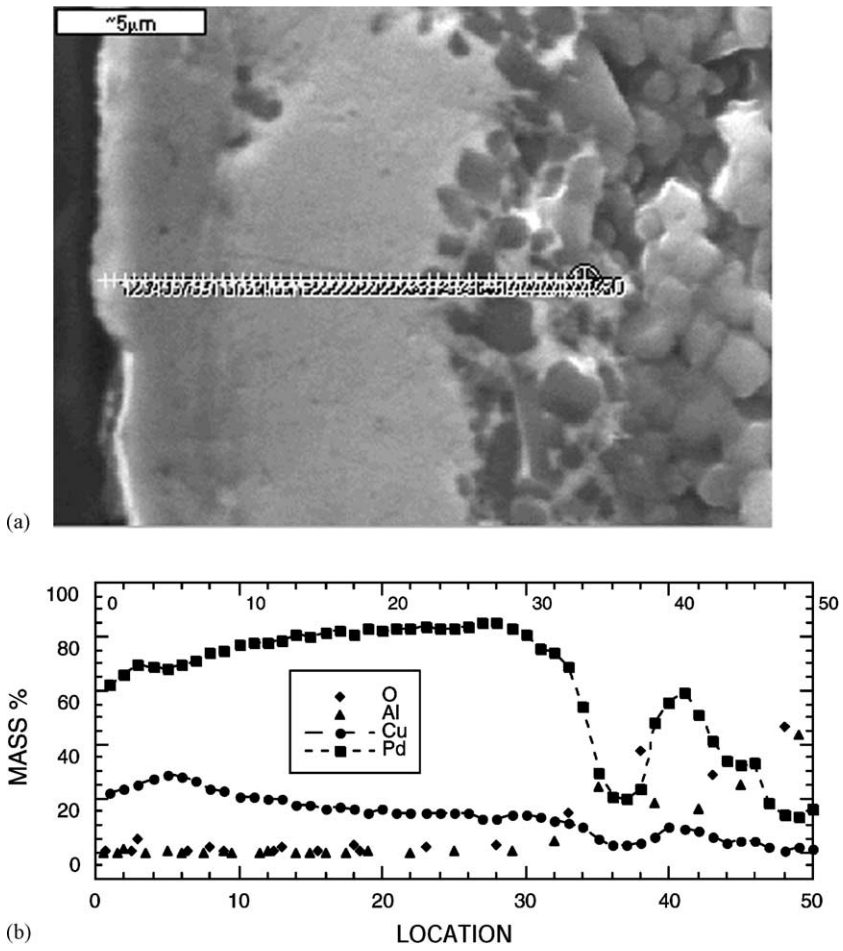

Fig. 6. Scanning electron micrograph (a) and EDAX analysis profile (b) for membrane 3. The crosses through the SEM image show the location of the individual EDAX analyses. Location 0 corresponds to the Pd–Cu membrane top surface and 50 corresponds to a point approximately 5 μm into the alumina support.

The improved performance of membrane 5 relative to membrane 3 could be due to the change in support structure or the difference in Cu composition of the metal film. The support structure changes include both a reduction in particle size cut-off (0.2–0.05 μm) and the use of an asymmetric support having lower resistance to flow. Both the support internal structure and the top layer pore size play fundamental roles in the membrane performance.

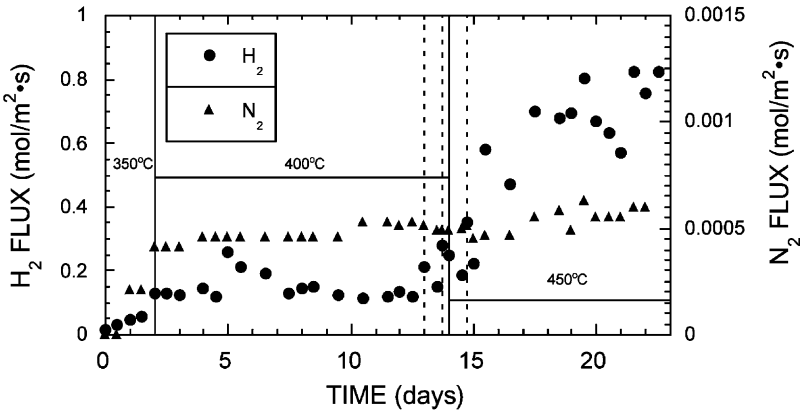

Fig. 7. Flux data for membrane 5. Metal layer thickness ≅ 10 μm. The pressure differential for permeation tests was 345 kPa. Dotted lines represent 30 min air purges.

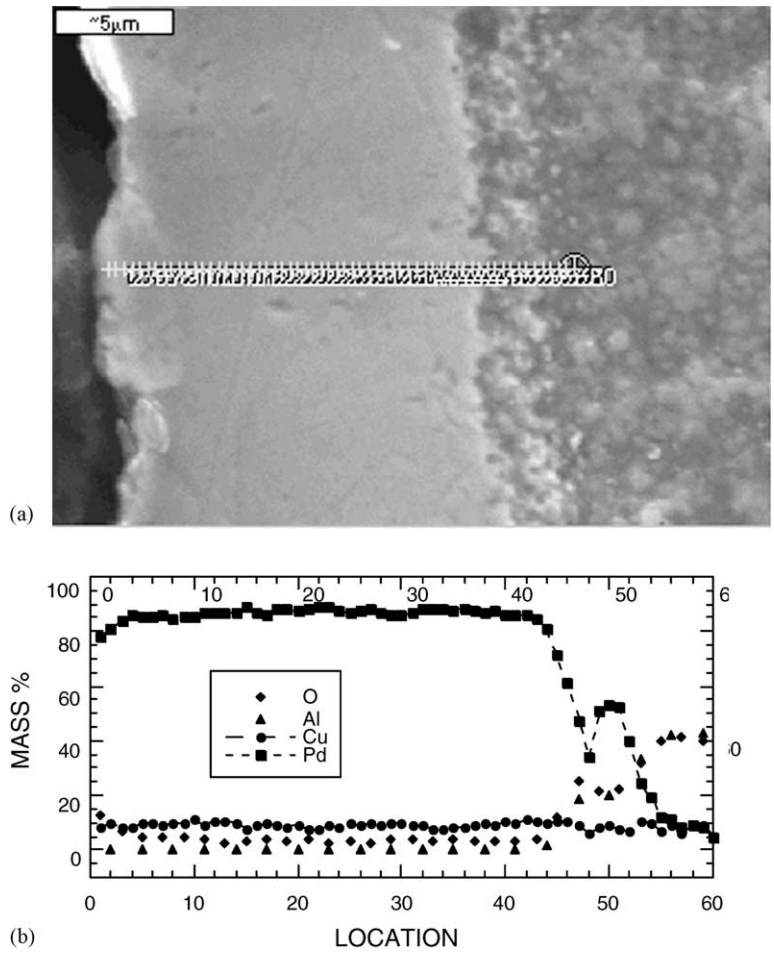

Fig. 8. Scanning electron micrograph (a) and EDAX analysis profile (b) for membrane 5. The crosses through the SEM image show the location of the individual EDAX analyses. Location 0 corresponds to the Pd–Cu membrane top surface and 50 corresponds to a point approximately 5 μm into the alumina support.

The asymmetric supports concentrate the mass transfer resistance in the top selective layer upon which the metal layer is deposited. This selective layer is very thin (less than 1% of the total wall thickness) as can be observed in Fig. 2. The inner layers are formed of increasingly larger particles of α-Al_2O_3 that offer small resistance to the flow. In contrast, the symmetric tubes used exhibit the same pore size all the way across the wall thickness. This type of support should present a considerably higher resistance to flow than asymmetric supports do as a consequence of that configuration. Thus, if a similar thickness of metal is deposited, greater fluxes can be achieved with the asymmetric support.

Regarding the large difference in separation factor, it is important to note the sizable differences in support pore size shown in Table 2. The asymmetric support used for membranes 5 and 6 had a pore size of 50 nm, while the analogous value for the symmetric tubes used for membranes 1 through 4 is 200 nm. The pore size is clearly related to surface roughness; a surface having small pores is smoother as a whole than another bearing large pores. On the smoother support, a more continuous metal film with fewer defects through which N_2 can diffuse is likely to result.

The above reasoning provides support for the hypothesis that a thinner film is required to make a leak-free membrane when a support with small pores is used. This is because it is relatively easier to cap small pores by plugging them with metal. Visible evidence that this occurs was observed in the SEM micrographs of membrane 5 as shown in Fig. 8. The metal penetrated into the pores of the support, filling them and then growing into a continuous thick layer of metal. The thickness of this layer appears to be more than adequate to produce a continuous film, suggesting that the thickness can be reduced even further. The next step was then to reduce the amount of metal deposited to verify this hypothesis.

Membrane 6 was made using the same asymmetric support used in membrane 5, but the total metal film thickness was only 1.5 μm. Fig. 9 shows the high temperature permeation behavior of this membrane and Fig. 10 is an SEM image of the metal layer. In observing the latter, it is important to highlight that even though the metal film was very thin in comparison with what has been reported in the

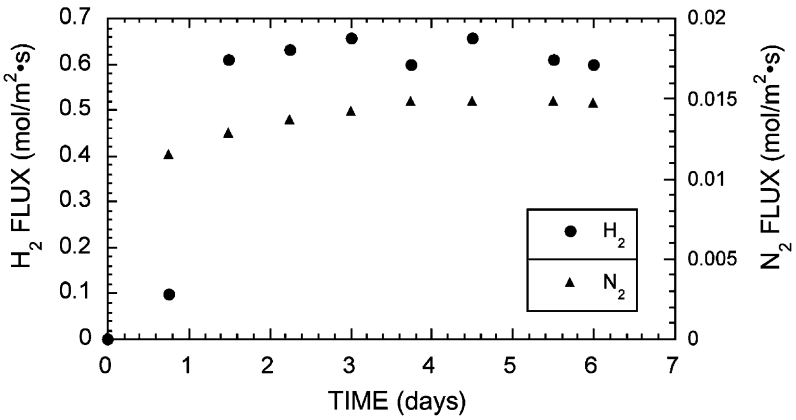

Fig. 9. Flux data for membrane 6. Film thickness ≅ 1 μm, temperature = 350 °C. The pressure differential for permeation tests was 345 kPa.

literature to date, it appears that a continuous film could be obtained with an even thinner film. However, the transport chart (Table 3 and Fig. 9) indicated an ideal H_2/N_2 separation was measured that was below the value for membrane 5. Still, membrane 6 compared well against all of the symmetric-supported membranes in terms of both flux and separation factor. An EDAX for this membrane showed a homogeneous composition of 30 wt.% Cu.

A reasonable explanation for the lower separation factor can be found by comparing the room temperature leak test results for membranes 5 and 6. According to the data in Table 2, the leakage rate for membrane 5 was slightly less than that of membrane 6 at room temperature. At high temperature however, membrane 6 leaked 18 times more nitrogen than did number 5 as inferred from the data in Table 3. Evidently, the thin metal film was enough to prevent leaking at low temperature, but when heated the metal crystallites may have sintered or otherwise rearranged, opening slightly covered pores in the ceramic support.

Membrane 7 was prepared on an even smoother asymmetric support having an γ-Al_2O_3 top layer, 5 nm in pore size. Several of these tubes were plated under the conditions outlined before, yet it was impossible to produce a leak-free membrane, even at thickness as high as 10 μm. As Lin and coworkers [46–48] have found, initial surface roughness is a critical factor for producing leak-free membranes. The supports used present large particles and other imperfections on the surface which the metal films could not cover up, as shown in Fig. 11. Also, we suspect the pores on this support to be so small as to not provide the interlocking required for the electrolessly deposited metal film to adhere strongly to the ceramic wall. Future work will include supports with an intermediate pore size between 5 and 50 nm that may exhibit sufficient surface roughness to provide adhesion between the support and the Pd–Cu film.

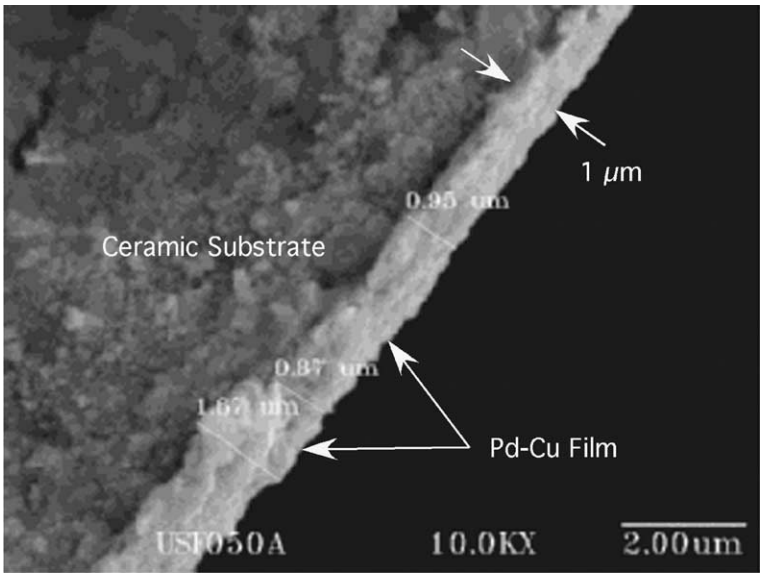

Fig. 10. Scanning electron micrograph of membrane 6. Scalebar is 2.0 μm.

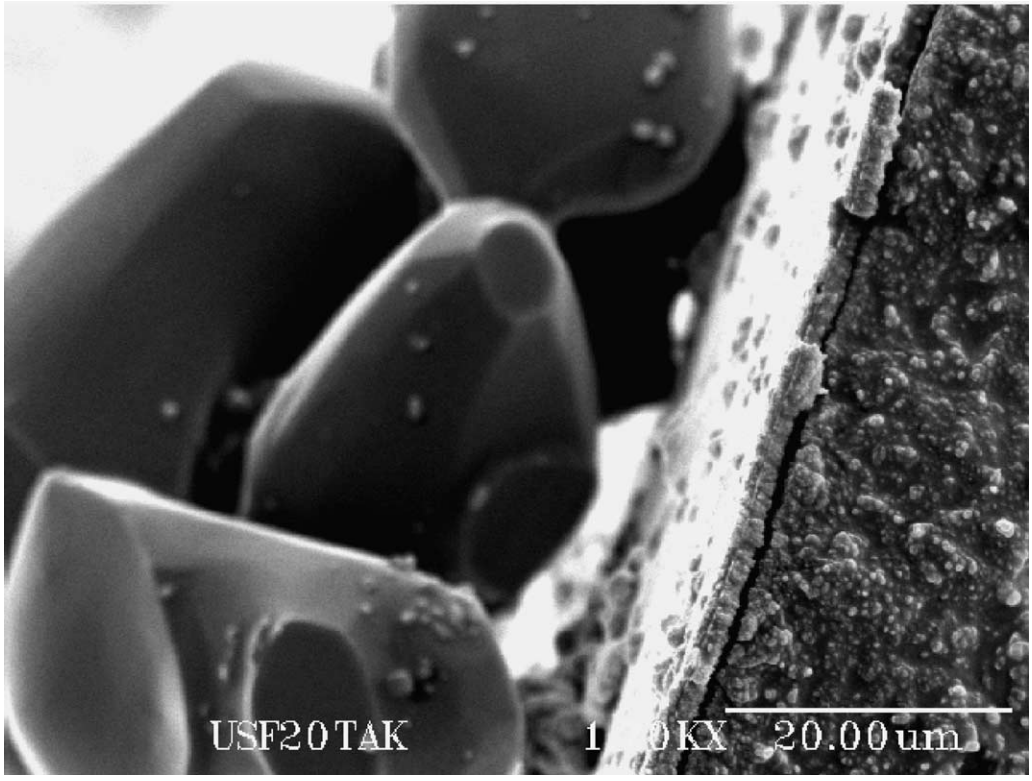

Fig. 11. Scanning electron micrograph of membrane 7. Scalebar is 20.0 μm.

4. Economics

The driving force towards thinner palladium–copper layers is twofold in nature. First, from a mass transport standpoint, thin metal films present less resistance to flow, giving higher flux as a result, therefore enhancing productivity. Second, less palladium is needed to produce the same amount of hydrogen per unit length. This last point is also addressed with the alloying of palladium with inexpensive copper. Both of these factors contribute enormously to the overall economics of the membrane manufacture. Employing supports with small pore size reduces the amount of expensive material needed to fabricate very selective leak-free membranes. Also, the use of asymmetric supports should reduce the overall mass transfer resistance, allowing more permeate production per unit area per unit time.

For better illustrating an application of these membranes, the following information, collected for design purposes, could be considered [58,59]. Several manufacturers are proposing to produce fuel cell power systems to produce 1 kW of electricity for residential use in Japan [59]. Production of 1 kW of electricity would require approximately 10 standard liters per minute (SLPM) of high purity hydrogen. Using membrane 6 as an example, 1.5 SLPM were produced using 5 cm of active length. Consequently, if the same type of Pd–Cu composite membrane were to be used, 30 cm of 1 cm OD membrane would be needed. The material costs to make the membrane are summarized in Table 4.

Table 4
Retail costs to make a 30 cm long section of a 2 μm thick Pd–Cu (Pd content 60 wt.%) membrane supported on an asymmetric ceramic ultrafilter

Item	Cost ($)
Asymmetric ceramic support	326
Palladium	6.5
Other chemicals	4.2
Electricity and supplies	0.2
Total	337.1

The bulk of the retail costs are associated with the support and not with the Pd film. A further decrease in the thickness would allow higher flux and would significantly lower the area requirements and length of support tubing needed. Several economical analyses have been carried out recently [60,61] indicating that the high cost of metal membrane devices for hydrogen separation is due mainly to palladium. Future economic analyses of this nature may need to consider the fabrication of micron-thick Pd films, which would significantly reduce the sensitivity of the economics to the cost of the Pd metal.

5. Conclusions

The objective of this work was to make ceramic-supported Pd–Cu metal membranes for high temperature hydrogen separation. It was shown that the deposition of Pd and Cu

using electroless plating followed by annealing to alloy the metals is a viable way of forming a thin homogenous and defect-free metal film capable of selectively separating hydrogen at temperatures between 350 and 700 °C.

Controlling the deposition time during the sequential electroless plating was found to be important to tailor the thickness and composition of the film. EDAX and XRD were used to analyze the alloy composition and the metal distribution throughout the metal film.

Two support structural factors were found to have an important impact on the overall performance of the membrane. The top layer pore size determines the minimum value the metal film thickness must be in order to prevent leaking and inert gas slippage. The larger the pore size the thicker the metal layer has to be to insure an impervious membrane. However, there is a limit in how small the film can be. Although our synthetic procedures were successful for 200 and 50 nm substrates, we were unable to deposit a free leak film on the 5 nm cut-off γ-alumina support.

The other important factor is the internal structure of the ceramic support. An asymmetric support, made of increasingly coarser layers, presents lower resistance to the flow, therefore yielding a higher hydrogen flux if compared with a symmetric one. The latter is homogeneous all the way across its thickness.

Using the electroless plating technique, it was possible to produce a palladium–copper composite membrane with average metal film thickness as small as 1.5 μm. The hydrogen flux of an 11 μm thick Pd–Cu film was 0.8 mol/m^2 s at 450 °C with a hydrogen/nitrogen ideal separation factor of 1150 at a ΔP of 345 kPa.

Acknowledgements

This work was supported by the US Department of Energy (DOE), University Coal Research Program under Grant no. DE-FG2699–FT 40585. The US Department of Energy (DOE) sponsored the portion of this work performed by Los Alamos National Laboratory. The authors are grateful to Prof. S. Uemiya of Gifu University for the generous donation of glass sealing powder. The authors also want to recognize Ms. Mary Anne Alvin and her colleagues from Siemens Westinghouse Power Corp. for her aid obtaining some of the SEM images and EDAX analyses.

References

[1] V. Gryaznov, Catal. Today 51 (1999) 391–395.
[2] R.E. Buxbaum, A.B. Kinney, Ind. Eng. Chem. Res. 35 (1996) 530–537.
[3] V.M. Gryaznov, M.M. Ermilova, S.I. Zavodchenko, N.V. Orekhova, Polym. Sci. 35 (1993) 365–368.
[4] N.M. Peachey, R.C. Snow, R.C. Dye, J. Membr. Sci. 111 (1996) 123–133.
[5] J.N. Armor, Catal. Today 25 (1995) 199–207.
[6] G. Saracco, H.W.J.P. Neomagus, G.F. Versteeg, W.P.M. van Swaaij, Chem. Eng. Sci. 54 (1999) 1997–2017.
[7] S. Uemiya, Sep. Pur. Meth. 28 (1999) 51–85.
[8] J.B. Hunter, Platinum Met. Rev. 4 (1960) 130–131.
[9] J.K. Ali, P. Hasler, E.J. Newson, D.W.T. Rippin, Int. J. Hydrogen Energy 19 (1994) 877–880.
[10] J.P. Collins, R.W. Schwartz, R. Sehgal, T.L. Ward, C.J. Brinker, G.P. Hagen, C.A. Udovich, Ind. Eng. Chem. Res. 35 (1996) 4398–4405.
[11] H.C. Foley, A.W. Wang, B. Johnson, J.N. Armor, ACS Symp. Ser. 517 (1993) 168–184.
[12] J.N. Armor, J. Membr. Sci. 147 (1998) 217–233.
[13] G.J. Grashoff, C.E. Pilkington, C.W. Corti, Platinum Met. Rev. 27 (1983) 157–169.
[14] J.B. Hunter, US Patent 2,773,561 (1956).
[15] D.L. McKinley, US Patent 3,439,474 (1969).
[16] D.T. Hughes, I.R. Harris, J. Less-common Met. 61 (1978) 9–21.
[17] W. Juda, C.W. Krueger, R.T. Bombard, US Patent 6,103,028 (2000).
[18] V.M. Gryaznov, A.P. Mishchenko, V.P. Polyakova, N.R. Roshan, E.M. Savitskii, V.S. Smirnov, E.V. Khrapova, V.I. Shimulis, Dokl. Akad. Nauk SSSR 211 (1974) 624–627.
[19] D.L. McKinley, US Patent 3,350,845 (1967).
[20] D. Edlund. A membrane reactor for H_2S decomposition, in: Proceedings of the Advanced Coal-fired Power Systems '96 Review Meeting, 1996, Morgantown, WV.
[21] F.N. Berseneva, N.I. Timofeev, A.B. Zakharov, Int. J. Hydrogen Energy 18 (1993) 15–18.
[22] D. Edlund, D. Newbold, C. Frost, US Patent 5,645,626 (1996).
[23] D.J. Edlund, EP Patent 783,919 (1997).
[24] F.A. Lewis, The Palladium Hydrogen System, Academic Press, London, 1967.
[25] J. Völkl, G. Alefeld, Hydrogen in Metals. I. Topics in Applied Physics, Vol. 28, Springer, New York, 1978.
[26] J. Piper, J. Appl. Phys. 37 (1966) 715–721.
[27] A.G. Knapton, Platinum Met. Rev. 21 (1977) 44.
[28] A.S. Zetkin, G.Y. Kagan, Y.S. Levin, Phys. Met. Metall. 64 (1987) 130–134.
[29] A.S. Zetkin, G.E. Kagan, A.N. Varaksin, E.S. Levin, Sov. Phys. Solid State 34 (1992) 83–85.
[30] R.A. Karpova, I.P. Tverdovskii, Russ. J. Phys. Chem. 33 (1959) 1393–1400.
[31] T.B. Flanagan, D.M. Chisdes, Solid State Commun. 16 (1975) 529–532.
[32] D. Fisher, D.M. Chisdes, T.B. Flanagan, J. Solid State Chem. 20 (1977) 149–158.
[33] M. van Swaay, C.E. Birchenall, AIME Trans. 218 (1960) 285–289.
[34] A.N. Karavanov, V.M. Gryaznov, Kinet. Catal. 25 (1984) 60–62.
[35] A.P. Mischenko, V.M. Gryaznov, V.S. Smirnov, E.D. Senina, I.L. Parbuzina, N.R. Roshan, V.P. Polyakova, E.M. Savitsky, US Patent 4,179,470 (1979).
[36] G. Barbieri, V. Violante, E. Drioli, Ind. Eng. Chem. Res. 36 (1997) 3369–3374.
[37] J. Shu, B.P.A. Grandjean, E. Ghali, S. Kaliaguine, J. Membr. Sci. 77 (1993) 181–195.
[38] S. Uemiya, T. Matsuda, E. Kikuchi, J. Membr. Sci. 56 (1991) 315–325.
[39] H. Kikuchi, Japan Patent JP 63,294,925 (1988).
[40] J.N. Keuler, L. Lorenzen, R.D. Sanderson, V. Prozesky, W.J. Przybylowicz, Nucl. Instr. Meth. Phys. Res. B 158 (1999) 678–682.
[41] K.Y. Foo, MS Thesis, Colorado School of Mines, Golden, CO, 1995.
[42] K. Hado, E. Yasumoto, K. Gamo, Japan Patent JP 9,029,079 (1997).
[43] O. Sakai, S. Nakamura, T. Kawae, H. Yoshida, Japan Patent JP 8,266,876 (1996).
[44] E. Kikuchi, S. Uemiya, Gas Sep. Purif. 5 (1991) 261–266.
[45] T. Kawae, T. Takahashi, O. Sakai, Japan Patent JP 10,203,802 (1998).
[46] V. Jayaraman, Y.S. Lin, M. Pakala, R.Y. Lin, J. Membr. Sci. 99 (1995) 89–100.
[47] G. Xomeritakis, Y.S. Lin, J. Membr. Sci. 133 (1997) 217–230.

[48] B. McCool, G. Xomeritakis, Y.S. Lin, J. Membr. Sci. 161 (1999) 67–76.
[49] K.L. Yeung, A. Varma, AIChE J. 41 (1995) 2131.
[50] K.L. Yeung, J.M. Sebastian, A. Varma, Catal. Today 25 (1995) 231–236.
[51] D.J. Edlund, US Patent 5,498,278 (1996).
[52] J.P. Collins, J.D. Way, Ind. Eng. Chem. Res. 32 (1993) 3006–3013.
[53] S.N. Paglieri, K.Y. Foo, J.D. Way, J.P. Collins, D.L. Harper-Nixon, Ind. Eng. Chem. Res. 38 (1999) 1925–1936.
[54] S.N. Paglieri, Ph.D. Thesis, Colorado School of Mines, Golden, CO, 1999.
[55] S. Aggarwal, A.P. Monga, S.R. Perusse, R. Ramesh, V. Ballarotto, E.D. Williams, B.R. Chalamala, Y. Wei, R.H. Reuss, Science 287 (2000) 2235–2237.
[56] T.B. Massalski, J.L. Murray, L.H. Bennett, H. Baker, L. Kacprzak, B.P. Burton, T. Weintraub, J. Bhansali (Eds.), Binary Alloy Phase Diagrams, Vol. 2, American Society for Metals, US, 1986, p. 1868.
[57] M. Kajiwara, S. Uemiya, E. Kikuchi, Catal. Today 56 (2000) 65–73.
[58] S. Thomas, Zalbowitz, Fuel Cells: Green Power, Los Alamos National Laboratory LA-UR-99-3231, 1999.
[59] T. Koppel, J. Reynolds, A Fuel Cell Primer: the Promise and the Pitfalls, Review 4 (September 15, 2000).
[60] A. Criscuoli, A. Basile, E. Drioli, O. Loiacono, J. Membr. Sci. 181 (2001) 21–27.
[61] S. Roy, B.G. Cox, A.M. Adris, B.B. Pruden, Int. J. Hydrogen Energy 23 (1998) 745–752.